buildings

MDPI

Article

Development of an FEM-DEM Model to Investigate Preliminary Compaction of Asphalt Pavements

Pengfei Liu [1,*], Chonghui Wang [1], Wei Lu [1], Milad Moharekpour [1], Markus Oeser [1,2] and Dawei Wang [1,3]

1   Institute of Highway Engineering, RWTH Aachen University, Mies-van-der-Rohe-Str. 1, 52074 Aachen, Germany; c.wang@isac.rwth-aachen.de (C.W.); wei.lu1@rwth-aachen.de (W.L.); moharekpour@isac.rwth-aachen.de (M.M.); oeser@isac.rwth-aachen.de (M.O.); wang@isac.rwth-aachen.de (D.W.)
2   Federal Highway Research Institute (BASt), Brüderstr. 53, 51427 Bergisch Gladbach, Germany
3   Yangzhou Deluda Transportation Technology Co., Ltd., Yangzhou 225000, China
*   Correspondence: liu@isac.rwth-aachen.de; Tel.: +49-241-80-20389

Abstract: Variations in pavement density have been widely monitored and investigated, both in laboratory and in field experiments, since the compaction of pavement is so critical to its long-term performance quality. In contrast to field testing, laboratory tests are simpler to produce but less accurate. Destructive drilled samples are used to conduct field testing; however, they are limited in their ability to assess density information at specific areas. The use of computationally aided approaches, such as the Finite Element Method (FEM) and the Discrete Element Method (DEM), in research involving asphalt mixtures is increasing, since these methods simulate and evaluate the characteristics of asphalt mixtures at macroscopic and microscopic scales. Individual particle behavior at the microscopic level cannot be fully represented using the FEM alone, and the computing cost of utilizing the DEM approach alone is prohibitively high. The objective of this work is to simulate the pre-compaction process by using the coupled FEM-DEM approach. In order to investigate the impact of the asphalt mixtures' gradation, a dense-graded asphalt mixture (AC 11) and a gap graded asphalt mixture (PA 11) were simulated. Different paving speeds (4, 5, and 6 m/min) were applied on the preliminary compaction model of AC 11 to study the effect of the paving speeds on the compaction process. By comparing the angular velocity, which worked as a reference of compaction quality, it was demonstrated that the grade AC 11 asphalt mixtures performed better in the preliminary compaction process compared to the grade PA 11 asphalt mixtures. Moreover, since it has an effect on compaction, paving speed was carefully monitored and kept within a reasonable range in order to maximize both pavement quality and project efficiency.

Keywords: FEM-DEM coupling method; pre-compaction; asphalt mixtures; machine-material interaction

1. Introduction

Asphalt pavement compaction is an essential step in the asphalt road construction process, affecting the strength and stability of the asphalt mixture and, as a result, the final road service quality and service life [1]. The field compaction process is typically divided into three stages: preliminary compaction, repeated compaction, and final compaction. The preliminary compaction process has a direct influence on the asphalt pavement, which should be compacted and stabilized to fulfill technical criteria and create favorable circumstances for the following steps [2]. The asphalt mix paver is used for the preliminary compaction process, which is to lay the asphalt mixture according to engineering technology specifications with a certain width and thickness uniformly on the base's surface, as well as to perform preparatory vibration compaction and screeding of the paving [3].

There are several different aspects that influence the compaction process, including the properties of the mixture composition, the environmental conditions, and the com-

paction method. As aggregate angularity, size, and hardness increase, the compactive effort required to achieve a given density increases [4]. During compaction, the gaps between the particles shrink as the air between the asphalt particles is continuously removed. It also means that the density of the pavement increases, which has been extensively measured and studied, both in laboratory experiments and field tests.

Existing investigations often employ traditional tests or imaging techniques to evaluate laboratory samples or drilled cores from field tests. For example, the X-ray computerized tomography (CT) scanning method has been widely employed due to its capacity to analyze the interior macroscopic characteristics of rock samples. It is also applied as an auxiliary tool for microscale petrography [5,6]. Later, non-destructive density gauges emerged, such as nuclear and non-nuclear gauges, to partially replace laboratory core measurements. Although the nuclear gauge's early concerns of being clumsy and heavy have been resolved, and its accuracy and operator safety have been enhanced, the need to have a license to operate this instrument must still be satisfied, which raises the threshold for administering lab tests. Nonnuclear gauges increasingly won over because of their user-friendly approach, speed, robust reproducibility, and slight standard variation across tests, as well as additional advantages such as ease of licensing [7,8]. Besides nuclear and nonnuclear gauges, ground-penetrating radar (GPR) [9,10] is a non-destructive testing tool that employs radar pulses to detect and picture conditions beneath the ground surface and is also frequently explored. Because of its high-speed, uninterrupted features, and the richness of pavement information it can provide, GPR is regarded as one of the most promising tools. However, the application of GPR to forecast the in-place density of asphalt mixtures is still in its early stages, and its performance requires further validation before it can be employed in practical situations [11,12].

However, both laboratory experiments and field tests have limitations. The data produced from laboratory experiments often deviate from the field tests, despite the ease of analysis and protection from interference. While the coring process can offer precise information regarding pavement density, it is irreversible and risks inflicting harm to the pavement and reducing its service life. In addition, the drilling of samples is done after the compaction of the pavement rather than during compaction. Gauges, whether nuclear or non-nuclear, are non-destructive. However, they must be artificially operated on the ground to collect relevant data, and they are subject to outside interference. Furthermore, these methods can only be used to measure and evaluate the pavement after the compaction work has been fully completed. In order to optimize the intervention timing, the ability to monitor or simulate in real-time the changes in the pavement condition during the time period between the paver paving and the roller compaction is desired.

Recently there have been a number of computationally assisted methods. Asphalt mixtures can be effectively simulated and studied during the paving process, such as analytical methods, continuum-based methods - finite element method (FEM), and discontinuity-based methods - discrete element method (DEM) [13,14]. These methods overcome the limitations of traditional research methods and are repeatable and stable simulation methods. The mechanical response of asphalt mixtures compacted by various ways was investigated using finite element simulations in the work by Liu et al. [15]. Experiments, digital image processing techniques, and FEM were used to compare and evaluate specimens produced using various compaction methods (including field compaction, Aachen compaction, and Marshall compaction). The Aachen compaction machine specimens were found to have a greater association with the field specimens than the specimens from the Marshall compaction. To explore the influence of compaction variables on air void distribution, Chen et al. used an open source DEM program to construct virtual digital specimens [16]. By preprocessing the particles and boundaries, the impacts of aggregate characteristics and compaction method on compaction were investigated, and the findings of the DEM simulation corresponded well with laboratory test results as well as data from the literature. In the study by Qian et al., the compaction process of asphalt mixtures was investigated by laboratory tests and DEM simulations. The meso structural changes of

asphalt mixtures were traced. Although the problem that the horizontal size distribution of particles is not entirely uniform still exists, it was confirmed that DEM simulation is an effective method to evaluate the compaction effect during compaction [17]. In addition, Wang et al. investigated the fundamental mechanics of asphalt compaction using FEM and DEM, respectively [18]. FEM was shown to accurately model the reduction of air voids. DEM can individually address the properties of each component, in contrast to FEM, which uses the continuum type modeling. DEM may, however, provide a rudimentary grasp of particle kinematics and relative binder-to-aggregate hardness. In addition, the mechanical properties of asphalt mixture samples produced by various compaction techniques may differ even if the degree of compaction is the same. There are, however, non-negligible limitations of both FEM and DEM when considering the interaction between asphalt mix and paver during real-time pre-compaction. When using a continuous method like FEM, the behavior of individual asphalt particles cannot be described in detail. When applying DEM, each asphalt particle is modeled as a separate entity, which is very suitable for studying phenomena occurring on the particle diameter length scale. However, the complex particle geometry and arrangement make the computational cost enormous.

The coupled FEM-DEM approaches are considered to improve the problems associated with the use of either method alone. One method of the FEM-DEM approaches is that the discrete elements are separated into independent finite element meshes, which considers each discrete element as a deformable continuum and separates them according to their existing discontinuity surface. Newton's second law determines the motion of individual components based on the unbalanced forces or unbalanced moments imparted on them. In contrast, the interaction between elements is governed by the contact transients between the blocks, which are processed in the same approach as the DEM. The deformation coordination criterion between elements is not required, and elements may be translated and rotated [19]. To describe the behavior of granular media, a rigorous hierarchical FEM-DEM coupling method was adopted by Guo and Zhao [20].It is illustrated that the proposed method can reproduce interesting experimental observations that are difficult to capture using traditional FEM or pure DEM simulations, such as the onset of the shear zone under smooth, symmetric boundary conditions, the noncoaxial particle response, the significant expansion and rotation at the shear zone's edge, and the critical state reached within the shear zone. Du et al. [21] created an innovative coupled FEM-DEM method to successfully simulate the numerical analysis of the Solid Grain Media Forming (SGMF) technological process. For the first time, it addressed the issue of elastic-plastic mechanics, the contact between a continuum and a discontinuity. Moreover, Orosz and Zwierczyk [22] investigated coupled FEM-DEM simulations of railroad sleepers in the instance of gravel roadbeds, revealing patterns in the stress state of concrete sleepers under typical loading.

In order to monitor the interaction between the material and the paving equipment, a modelling methodology was developed in this study through a coupled FEM-DEM method. The general-purpose FE software ABAQUS was used for the modelling. FEM was used in large areas of this simulation, in this case the pavement base and the paver, and DEM in smaller, more localized areas, here was the asphalt mixture component. In particular, each DEM particle representing an aggregate in the preliminary compaction was modeled with a single-node element. These elements were rigid spheres with specified radii and had displacement and rotational degrees of freedom. General contact definitions were extended to include interactions among DEM particles and interactions between DEM particles and FE-based (or analytical) surfaces. In the following sections, the process of preliminary compaction modelling is described in detail. After many attempts, the optimal modelling parameters are determined, and the results generated by the numerical simulations are compared between the actual situation and previous studies, which involved the influence of factors such as different material parameters of the asphalt mixture and different operating parameters of the paver. Based on the results and discussion, conclusions are drawn, which is beneficial to further investigation on the material compaction behavior and its mechanical performance afterwards. It is worth mentioning that as preliminary research

for simulating the compaction, some simplifications and assumptions were adopted in the FEM-DEM coupled method. The actual shapes of the aggregates were instead uniformly substituted by spheres, which decreases the degree to which the simulation is accurate in comparison to the real scenario to some extent. In addition, ambient temperature and wind velocity are supposed to be considered in the simulation to get close to the real condition of pavement construction. These limitations should be considered for future research.

2. Modelling of Preliminary Compaction Based on FEM-DEM Coupled Method

In this chapter, the detailed modeling process of the preliminary compaction in ABAQUS will be introduced. ABAQUS is one of the world's most advanced nonlinear finite element software and provides a simple uniform interface for creating, submitting, monitoring, and analyzing simulation results. It has progressed to the point where discrete element simulation is now available with this finite element simulation program [23]. The simulation flowchart is shown in Figure 1. Some main steps of the modelling procedure will be introduced in the following sections.
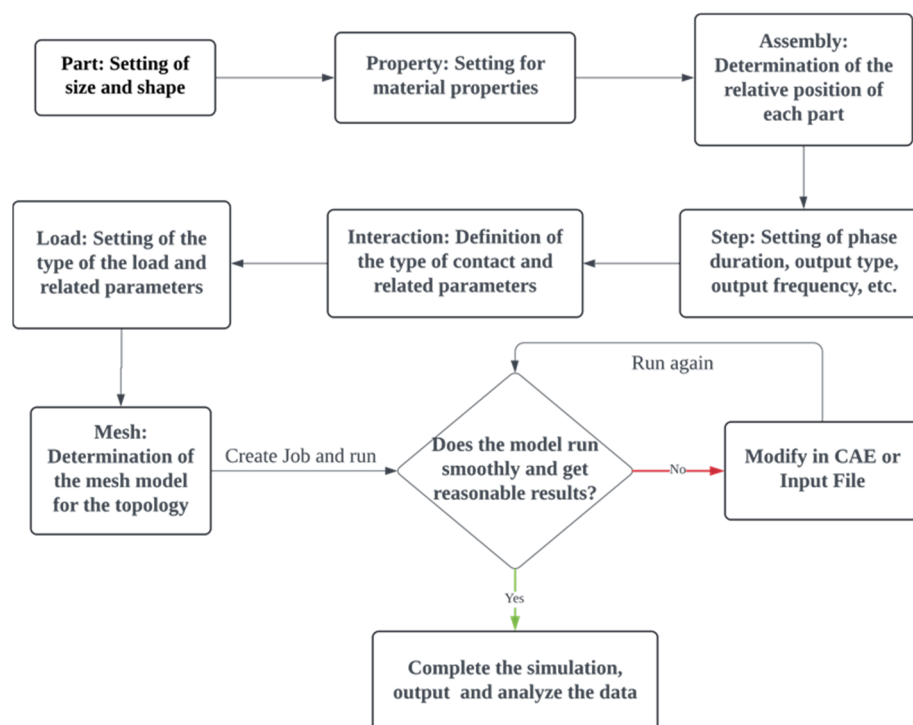

Figure 1. Flowchart of the FEM-DEM coupled modeling.

2.1. Creation of the Different Parts of the Model

One of the key parts of the compaction model is the aggregates, which were generated by the particle generator in ABAQUS. The particle generator enables a modeling technique in which the DEM is checked only when the particles reach a defined area, which simplifies the construction of the model while improving the computational efficiency [24]. The particles are released in a direction perpendicular to the inlet surface of the particle generator and the flow rate should be determined according to the paving speed. In this study, only one particle generator was used. In order to improve the computational efficiency, the morphology of the aggregates was simplified to spheres, which cannot fully simulate the aggregate interlocking happening during compaction. The approach to simplify the geometry of the aggregates while keep their main features will be studied in the future. The element type of particles released by the particle generator was PD3D, representing discrete particles. In order to investigate the influence of the gradation of the asphalt mixture on the pre-compaction, two different asphalt mixtures, a dense-graded mixture AC11 and a gap graded mixture PA11, were simulated and their gradations are shown in Figure 2.
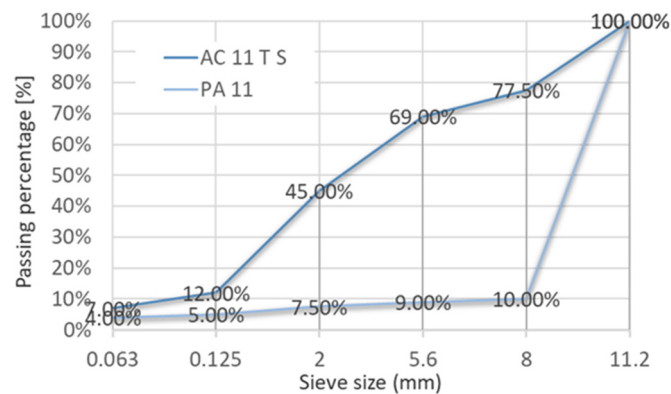
Figure 2. Grading Curve of AC 11 and PA 11.

The distribution of the particles size was controlled by a probability density function (PDF). Different forms of probability density functions, such as uniform, normal, lognormal, piecewise linear, and discrete distributions, are supported by the particle generator. In this case, discrete distributions were used in the PDF. The three largest size levels in the gradation were taken into account in the simulation, and the maximum number of the particles to be released was set as 10,000 based on trade-offs between accuracy and computational cost. The density of the aggregates was set to 2.85×10^{-9} ton/mm^3, and the Young's modulus and Poisson's ratio were set to 20,800 MPa and 0.3, respectively.

In this study, the other parts including the base and the paver were created and discretized by FEM. The base that was ready to be compacted on by the paver was simplified to a shell 3.42 m wide and 17.14 m long without thickness, on which two shells 0.4 m high and around 1.14 m apart were created as a fence to designate the paver's work path. As a result of the impact of vibration paver vibration, the unit line pressure is greatly improved, and when the vibration paver continues to make rapid impact on the surface, the same frequency of pressure waves penetrates into the material layer, causing the material particles to move, rearrange, and become denser as a result. Therefore, vibratory pavers are becoming more popular and will be used in this model. The paver has been diminished to its two most fundamental components: the tamper and screed. When the tamper portion was set as indicated in Figure 3, the screed was set as a hollow rectangle with a length of 1.27 m, a width of 1.07 m, and a height of 0.72 m. Since the base, tamper, and screed are assumed as rigid bodies, they do not need to be assigned any material properties.
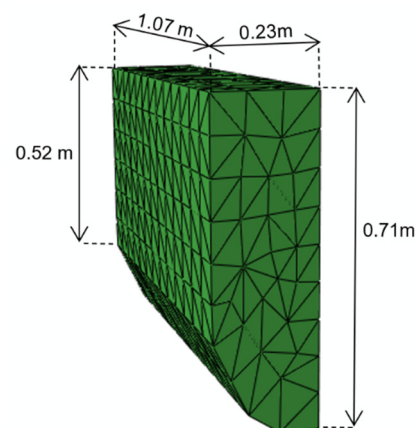

Figure 3. Tamper.

2.2. Assembly of the Different Parts and Their Interaction

The parts including particle generator, the base, and the paver were assembled together in ABAQUS. As shown in Figure 4, the paver was placed on the far right side of the base

and screed to the left in the forward direction. The tamper and the part generator were placed in the middle of the specified route. The distance between the lowest point of the tamper and the screed and the base was set at 0.4 m, which was the thickness of the asphalt mixture initially required to be paved. In front of the paver, a particle generator serves as both an unloading truck and as paver blades. The particle generator has almost the same width as the paver body, ensuring that the particles are equally distributed over the road to be paved. Furthermore, it is located near to the base (approximately 48 cm), ensuring that the asphalt particles do not bounce hard on the base after being released owing to their high velocity, but leaving enough space for the particles to aggregate on the base.
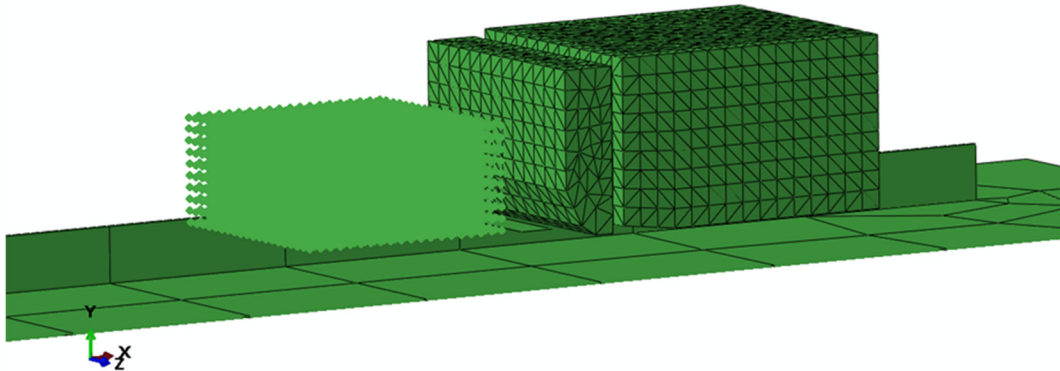

Figure 4. The assembled model.

The coordinate system of the model should be referred to in order to sort out the subsequent directions to which the data refers. As shown in the Figure 4, the negative direction of x is the forward direction of the paver; the negative direction of y is the direction of the falling asphalt particles; and the z direction is perpendicular to the forward direction of the paver in the horizontal direction.

The contact between particle and tamper, particle and screed was simplified as Hertzian contact [25], defined with a limit value of Hertzian stiffness of 2000 MPa and a friction coefficient of 0.7. To prevent the particles from moving away from the base due to the paver's activity, or from sliding on the base, the connection between the particles and the base should include an extra force based on the Hertzian contact that causes the particles to cling to the base. As a result, the contact type between the particles and the base was set to the JKR model [26], with a surface energy of 10 mJ per unit area limit value of stiffness of 100 MPa and a friction coefficient of 0.95. Also, the contact type between the particle and the particle was set to the JKR model, with a surface energy of 10 mJ per unit area, limit value of stiffness of 100 MPa, and a friction coefficient of 0.65. The JKR model was proposed by Johnson, Kendall, and Roberts in 1971, and allows for tensile forces to develop due to surface adhesion. It is widely used to describe viscous contacts, and therefore the JKR model was used in this study.

2.3. Definition of the Computational Steps and Boundary Conditions

Since the model required the observation of pavement condition changes before and after initial compaction, a certain length of the pavement that the paver was working steadily on could be observed, which meant that the duration of the step needed to be sufficient for the paver to travel over the specific area. Additionally, the step time is proportional to the paver's forward speed. The speed of the tamper and the screed were both set at speeds of 4 m/min, 5 m/min, 6 m/min to investigate the effect of the paving speed on the paving process. Furthermore, the screed and tamper were set to a periodic, uniform amplitudes of 1 cm and 0.8 cm, with frequencies of 20 Hz and 30 Hz, respectively, which enabled the pavement to be compacted and screeded to increase its compactness, reducing the number of compaction passes by the roller and improving the pavement's surface quality.

3. Results and Discussion

3.1. Illustration of the Paving Process

The asphalt mixtures AC 11 underwent obvious changes after the initial compaction by the paver, which can be seen in Figure 5; the air voids between the asphalt particles became narrower, while the surface of the asphalt layer became smoother.
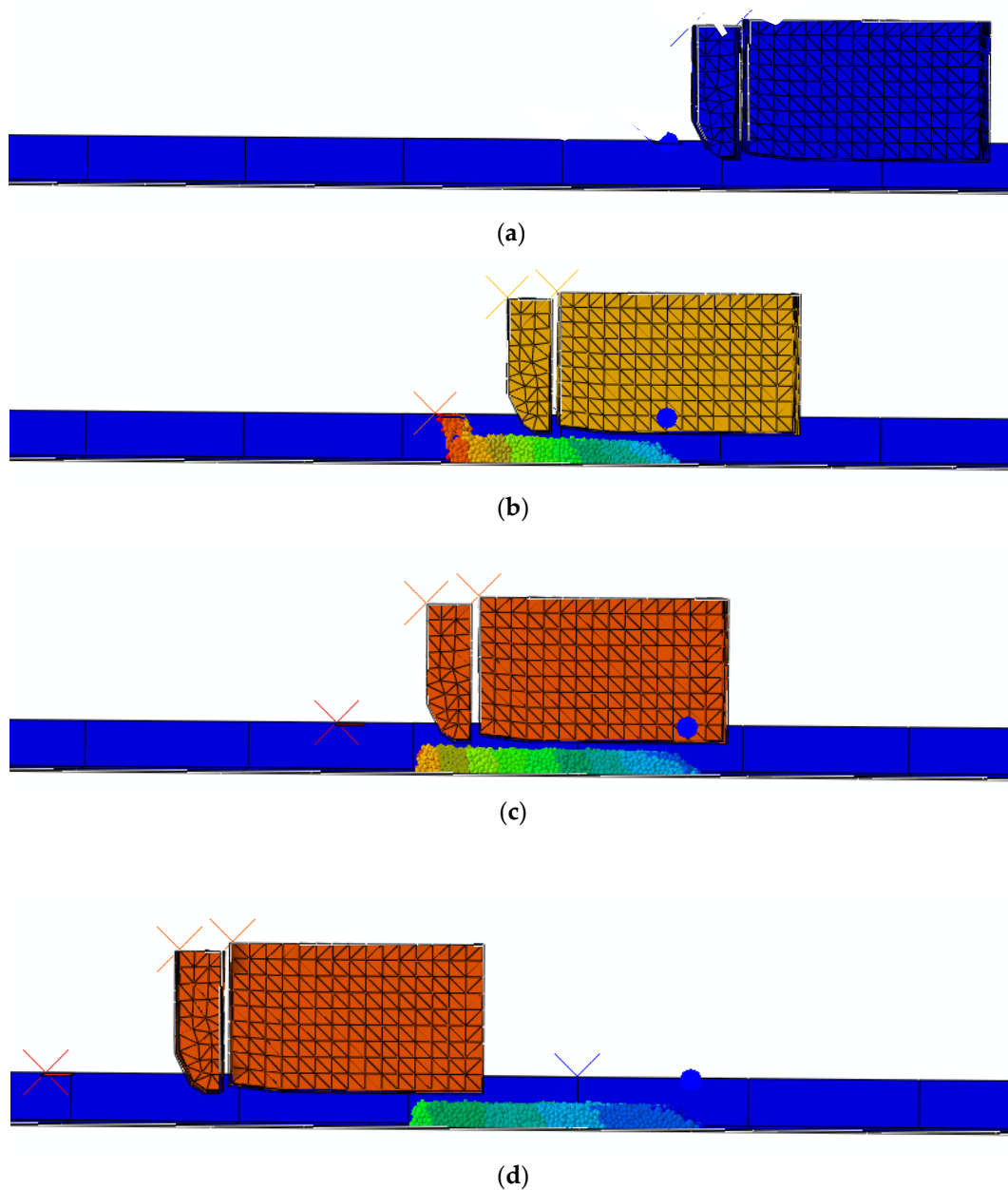

(**a**)

(**b**)

(**c**)

(**d**)

Figure 5. Three steps of this model: (**a**) The beginning of step 1 (t = 0); (**b**) The end of step 1, the beginning of step 2 (t = 2 s); (**c**) The end of step 2, the beginning of step 3 (t = 3 s); (**d**) The end of step 3 (t = 6 s).

Particularly, step 1 was initiated when the paver started moving forward and the particle generator started releasing particles, which lasted for 2 seconds; then it went to step 2, which lasted for 1 second and during which the required number of particles had been fully released. Finally, in step 3, in order to observe the state of the asphalt layer after being acted upon by the paver, the paver still needed to move forward at a constant speed until a certain part of the fully acted upon particles was exposed. In this process, only step 2, which took a one-second time interval, was necessary to produce data pertaining

to the paver's contact with the asphalt particles at a high frequency, while steps 1 and 3 required essentially minimal data output.

In order to assess the interaction between asphalt particles and pavers, the relative rotation pattern of particles was chosen to evaluate, because it strongly relates to the density fluctuation of the mixture [27], i.e., the preliminary compaction could be accomplished by pressing and compacting particles while their aggregates are continually rotating and rearranging, until the particles reach a stable state, and thus the degree of compaction can be determined by observing the relative rotational behavior of the particles [28].

3.2. Effect of the Gradation of Asphalt Mixtures on the Paving Process

There are a variety of factors that can influence the compaction properties of asphalt mixtures, including grading, temperature, bitumen content, aggregate qualities, compaction procedures, and other variables [29]. In order to examine the influence of gradation on the compaction characteristics of asphalt mixtures, two kinds of asphalt mixtures, AC 11 and PA 11, both with a maximum particle size of 11.2 mm, were used in this study. Ten particles that would be impacted by the paver in step 2, described in the last section, were chosen. Their rotating motions during compaction were observed, and the angular velocities of their rotational axes in three directions were plotted in Figures 6–9. In these figures, each curve representing the corresponding angular velocity of each particle is drawn in specific color.
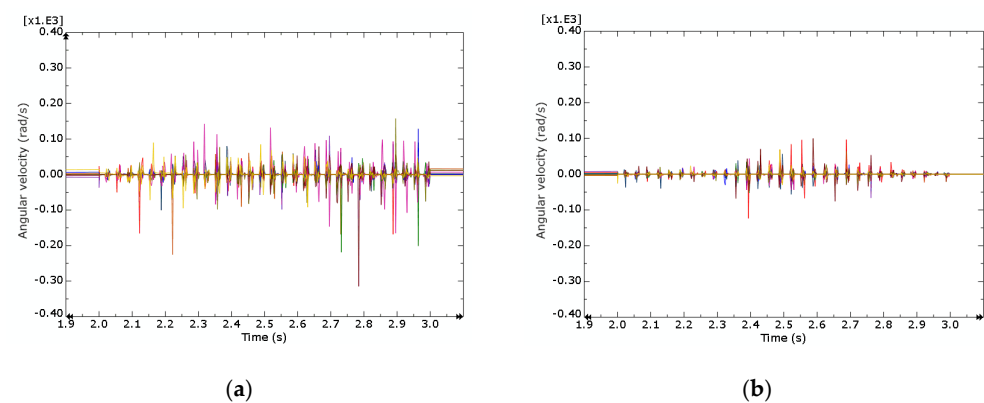

(**a**)   (**b**)

Figure 6. Angular velocity of different mixtures: (**a**) AC 11 in X-direction; (**b**) PA 11 in X-direction.
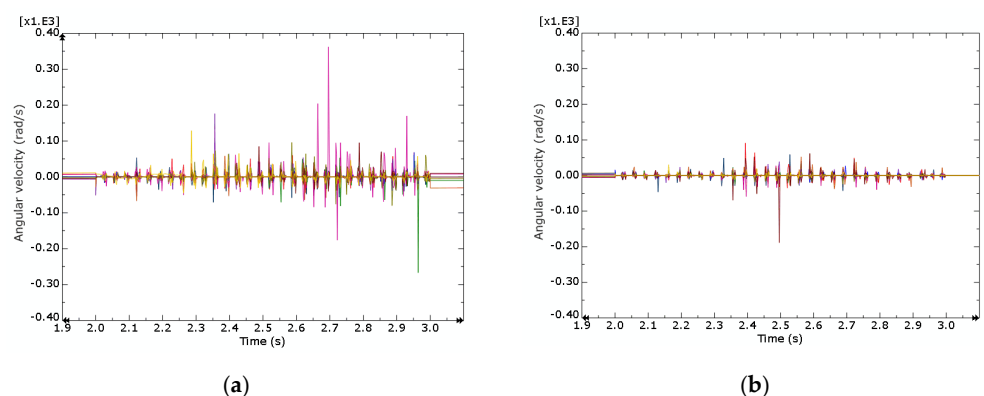

(**a**)   (**b**)

Figure 7. Angular velocity of different mixtures: (**a**) AC 11 in Y-direction; (**b**) PA 11 in Y-direction.

Eight data plots can be found in Figures 6–9, where the X-axis represents the time in s, and the time interval from 2.0 s to 3.0 s is chosen, i.e., the time period during which step 2 was performed. The Y-axis represents the angular velocity in rad/s, and the interval chosen after observation is from −0.4 rad/s to 0.4 rad/s. As shown in these figures, during the paving process, the angular velocity of the aggregates fluctuated quickly; this fluctuation is mostly driven by the high frequency of vibration from the paver screed. The peak in the graph indicates that the angular velocity of the aggregate is at its maximum at this

point, which means that the paver is acting on this aggregate. As can be seen from the graphs with combined angular velocity, the fluctuation of the angular velocity of AC 11 is generally more significant than the fluctuation of the angular velocity of PA 11: both the angular velocity variation in each direction and the total angular velocity variation show more frequent peaks in the graphs related to the angular velocity of the AC 11 aggregate than in the graphs related to the angular velocity of the PA 11 aggregate.
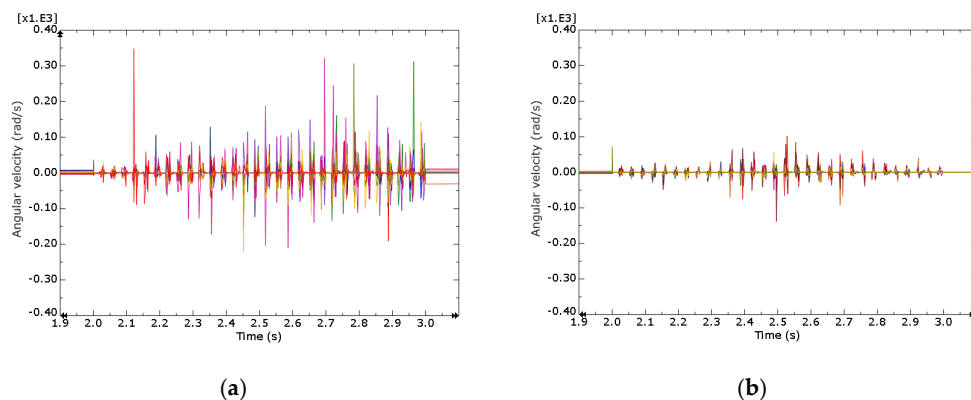

Figure 8. Angular velocity of different mixtures: (**a**) AC 11 in Z-direction; (**b**) PA 11 in Z-direction.
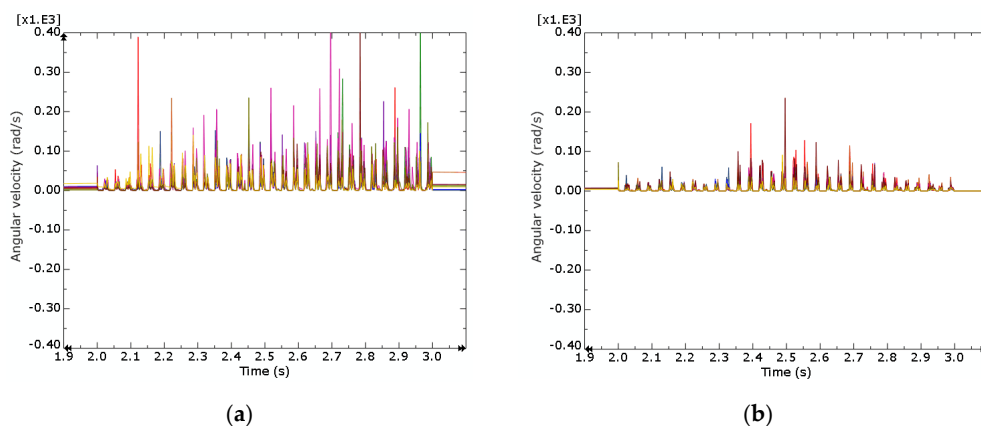

Figure 9. Combined angular velocity of different mixtures: (**a**) AC 11; (**b**) PA 11.

Specifically, Figure 6 shows the angular velocities of asphalt particles of AC 11 and PA 11, respectively, rotating in the X direction as the axis. After comparison, it can be seen that the rotation of the asphalt particles with grade AC 11 is more intense, with the maximum rotational angular velocity fluctuating between −0.3 rad/s and 0.15 rad/s, while the rotation of the asphalt particles with gradation PA 11 is relatively gentle, with the maximum rotational angular velocity fluctuating between −0.15 rad/s and 0.1 rad/s.

Figure 7 displays the angular velocities of the asphalt particles rotating in the Y direction for AC 11 and PA 11, respectively. Most of the particles of both grades rotate relatively gently in the Y-direction, floating between −0.1 rad/s and 0.1 rad/s. Only a few asphalt particles of grade AC 11 rotated more vigorously with a maximum angular velocity of 0.35 rad/s, as well as a much smaller number of asphalt particles of gradation PA 11 with a maximum angular velocity of −0.2 rad/s.

Figure 8 shows the angular velocities of asphalt particles of AC 11 and PA 11, respectively, rotating in the Z direction as the axis. After comparison, it can be seen that the rotation of the asphalt particles with grade AC 11 is more intense, with the maximum rotational angular velocity fluctuating between −0.3 rad/s and 0.15 rad/s, while the rotation of the asphalt particles with gradation PA 11 is relatively gentle, with the maximum rotational angular velocity fluctuating between −0.15 rad/s and 0.1 rad/s.

Figure 9 demonstrates the combined angular velocities of the asphalt particles of the two gradations in all directions. The combined angular velocity is defined as the root of the sum of squares of angular velocities in three directions. It can be clearly seen that the particles of AC 11 gradation are more active, and some of them even reach the maximum rotational angular velocity of 0.4 rad/s, while the particles of PA 11 gradation generally move more slowly with the rotational angular velocity within 0.25 rad/s.

As a result, it can be seen that different gradation conditions have different effects on the preliminary compaction when other conditions remain constant. Also, the asphalt particles with grade AC 11 are more active than those with grade PA 11, which means that when the former are used in the preliminary compaction process, the compaction effect is relatively better.

3.3. Effect of the Paving Speed on the Paving Process

The paving speed has an effect on the length of time it takes the paver to compress a unit area of material. When compacting the surface layer of asphalt mixture, the paver cannot change the paving speed, and should avoid stopping in the middle. Furthermore, unequal paving pace might result in uneven surface roughness, which can have an impact on compaction and smoothness. In the study of the effect of paving speed on the preliminary compaction process and the degree of compaction, the AC 11 material was used with speeds of 4 m/min, 5 m/min, 6 m/min, and run through the model, and the results are shown in Figures 10–12, respectively.
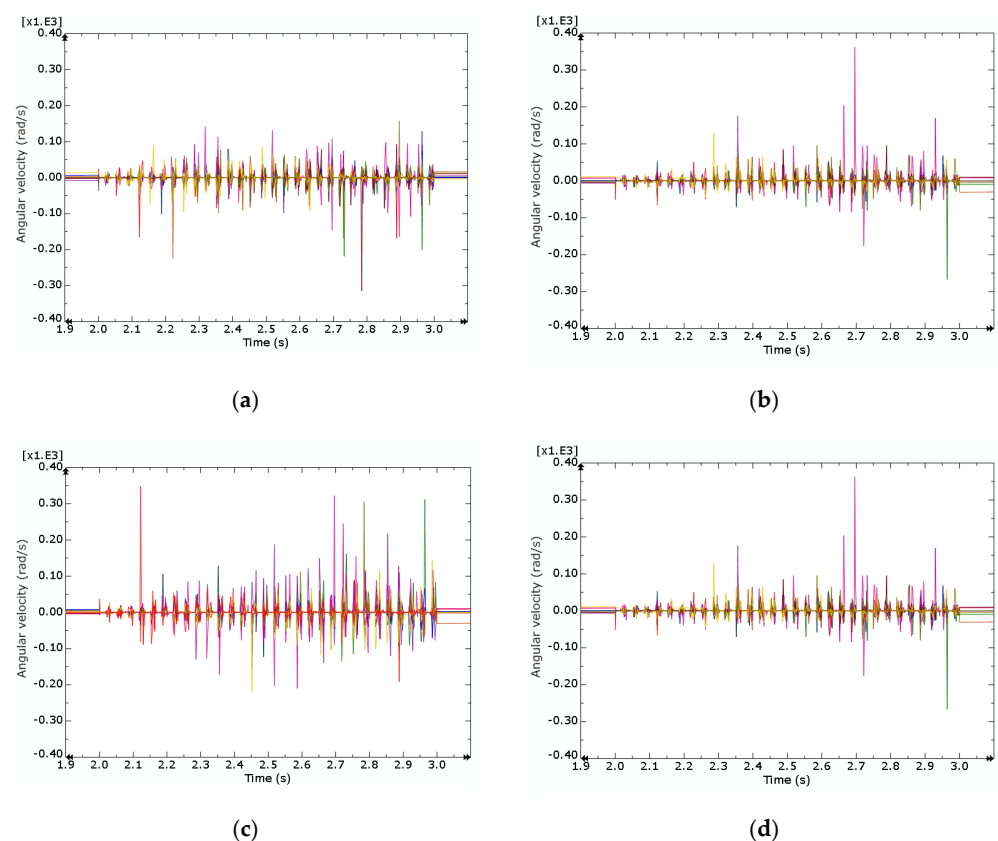

(**a**)

(**b**)

(**c**)

(**d**)

Figure 10. Angular velocity of AC 11 aggregate with a paving speed of 4 m/min: (**a**) in X-direction; (**b**) in Y-direction; (**c**) in Z-direction; (**d**) combined angular velocity.

Figure 11. Angular velocity of AC 11 aggregate with a paving speed of 5 m/min: (**a**) in X-direction; (**b**) in Y-direction; (**c**) in Z-direction; (**d**) combined angular velocity.
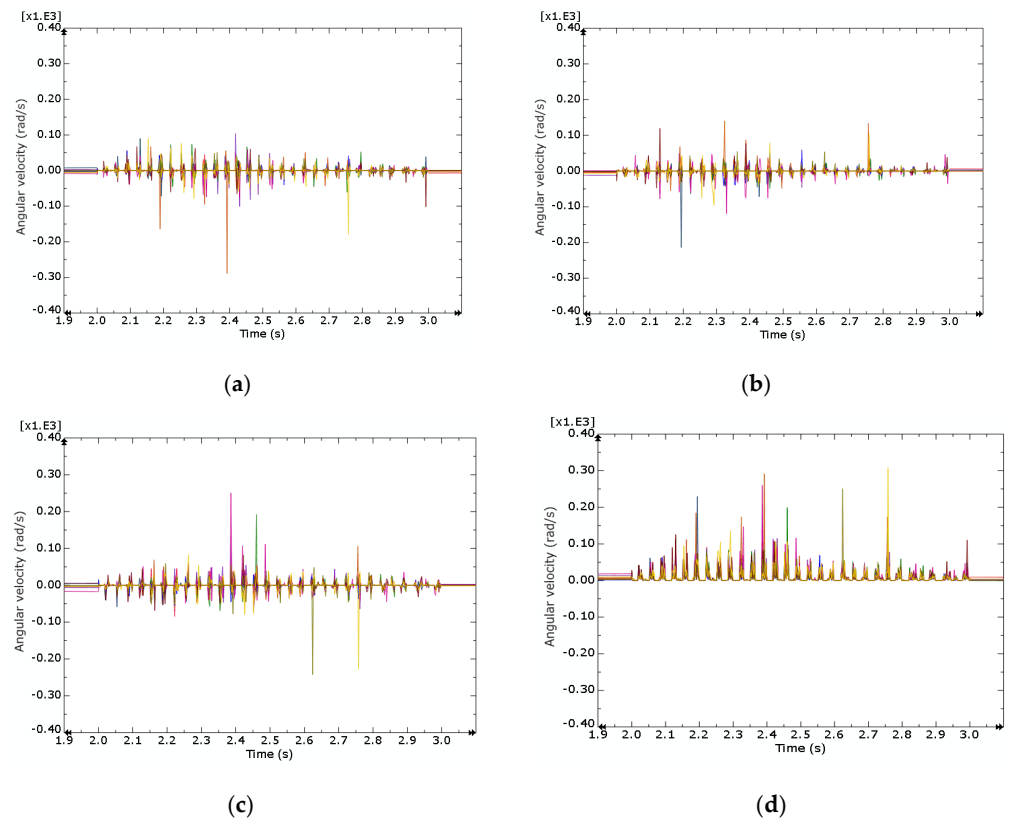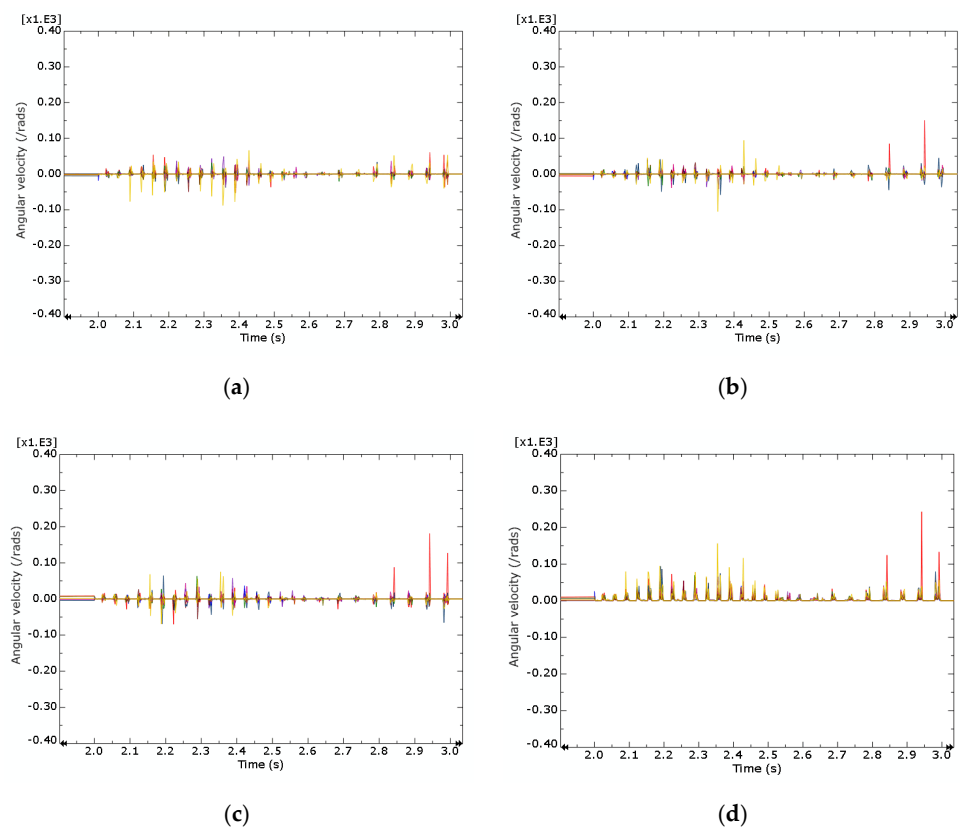
Figure 12. Angular velocity of AC 11 aggregate with a paving speed of 6 m/min: (**a**) in X-direction; (**b**) in Y-direction; (**c**) in Z-direction; (**d**) combined angular velocity.

The asphalt aggregate seemed very active when the paving speed was set to 4 m/min, with angular velocities oscillating between −0.4 rad/s and 0.4 rad/s, as indicated in the preceding subsection. When the speed was raised to 5 m/min while the other parameters remained constant, the angular velocity of the asphalt aggregate fell in all directions, with a maximum peak of 0.3 rad/s, indicating that the compaction was not as good as when the speed was set at 4 m/min. When the speed was raised again, to 6 m/min, the activity of the asphalt aggregate was relatively weak, with the angular velocity floating between −0.1 rad/s and 0.2 rad/s. The data generated with paving speed as a variable compared to [2], a similar pattern was found that if the paving speed is faster while keeping other conditions constant, the asphalt mixture will compact less during the preliminary compaction stage. The whole paving operation must be carried out at a constant pace without stopping in order to increase the mixture's evenness and to minimize segregation. In the case of heavy traffic, it is necessary to pave as quickly as possible and move on to the next process so that the road can be put into service as quickly as possible. As a result, paving should be restricted to a reasonable speed range.

4. Conclusions and Outlook

Compaction is a critical step in the building of asphalt pavement; the quality of the asphalt pavement plays a significant role; both under-compaction and over-compaction will have an impact on the quality of the asphalt pavement; and numerous variables influence asphalt compaction, including material-related characteristics such as the gradation of the asphalt mixture and paver-related parameters such as the paving speed, and others. This paper uses a coupled FEM-DEM method to simulate the preliminary compaction process, considering the influence of the gradation of the asphalt mixture and the paving speed on the preliminary compaction process. By observing the angular velocity of the particles, it was concluded that the graded asphalt mixture with AC 11 aggregate could be better compacted by the paver compared with the PA 11 mixture, and the paving speed could be controlled within a suitable speed range to achieve a better trade-off between paving quality and project efficiency.

As preliminary research on the FEM-DEM coupled method for simulating the compaction, the data obtained from the model may differ from the actual situation for several possible reasons. For example, in this model, the asphalt mixture was only compacted one time under the action of the paver, while it is better to have more than two times in real situation. Thus, the compaction has not yet reached the required level. Another limitation is that the actual aggregates are not represented in the ABAQUS program, but are instead uniformly substituted by spheres, which decreases the degree to which the simulation is accurate in comparison to the real scenario to some extent. To conduct simulations with acceptable accuracy and low computational cost, the approach to simplify the geometry of the aggregates while keep their main features will be used to simulate the aggregates [30]. In addition, more factors, such as ambient temperature and wind velocity, are supposed to be considered in the simulation to get close to the real condition of pavement construction. Based on the information such as the characterization of aggregate skeleton derived from the preliminary compaction simulation, the final compaction by the roller compactor with finite deformation can be simulated by FEM, and the stability of the asphalt mixture can be predicted by the methodology proposed in [31]. Moreover, more parameters used to evaluate compaction will be presented; for example, the porosity of the material or the apparent density, and the evenness of the pavement. The ultimate research aim is to develop a mature numerical model for simulating the compaction process which can be applied in Building Information Modeling and Digital Twin for road construction and maintenance.

Author Contributions: Conceptualization, P.L.; methodology, C.W. and P.L.; software, W.L. and P.L.; validation, C.W. and M.M.; formal analysis, W.L.; investigation, W.L., C.W. and P.L.; resources, C.W. and M.M.; data curation, W.L.; writing—original draft preparation, W.L. and P.L.; writing—review and editing, P.L. and D.W.; visualization, W.L.; supervision, C.W., P.L. and M.O.; project administration, P.L. and M.O.; funding acquisition, P.L. and M.O. All authors have read and agreed to the published version of the manuscript.

Institutional Review Board Statement: Not applicable.

Informed Consent Statement: Not applicable.

Data Availability Statement: Data is available with the first author and can be shared with anyone upon reasonable request.

Conflicts of Interest: The authors declare no conflict of interest.

References

1.　Mo, L.; Li, X.; Fang, X.; Huurman, M.; Wu, S. Laboratory investigation of compaction characteristics and performance of warm mix asphalt containing chemical additives. *Constr. Build. Mater.* **2012**, *37*, 239–247. [CrossRef]

2.　Liu, P.; Wang, C.; Otto, F.; Hu, J.; Moharekpour, M.; Wang, D.; Oeser, M. Numerical simulation of asphalt compaction and asphalt performance. In *Coupled System Pavement-Tire-Vehicle*; Springer: Cham, Switzerland, 2021; pp. 41–81.

3.　Jia, J.; Liu, H.; Wan, Y.; Qi, K. Impact of vibration compaction on the paving density and transverse uniformity of hot paving layer. *Int. J. Pavement Eng.* **2020**, *21*, 289–303. [CrossRef]

4.　*AC 150/5370-14A*; Hot-Mix Asphalt Paving Handbook 2000. US Army Corps of Engineers: Washington, DC, USA, 2000.

5.　Nabawy, B.S.; David, C. X-ray CT scanning imaging for the Nubia sandstone as a tool for characterizing its capillary properties. *Geosci. J.* **2016**, *20*, 691–704. [CrossRef]

6.　Zhang, C.; Wang, H.; You, Z.; Yang, X. Compaction characteristics of asphalt mixture with different gradation type through Superpave Gyratory Compaction and X-ray CT Scanning. *Constr. Build. Mater.* **2016**, *129*, 243–255. [CrossRef]

7.　Sully-Miller Contraction, C.O. *A Summary of Operational Differences between Nuclear and Non-Nuclear Density Measuring Instruments*; TransTech Systems, Inc.: Schenectady, NY, USA, 2000; Volume 5.

8.　Van den Bergh, W.; Jacobs, G.; De Maeijer, P.K.; Vuye, C.; Arimilli, S.; Couscheir, K.; Lauriks, L.; Baetens, R.; Severins, I.; Margaritis, A.; et al. Demonstrating innovative technologies for the Flemish asphalt sector in the CyPaTs project. *IOP Conf. Ser. Mater. Sci. Eng.* **2019**, *471*, 022031. [CrossRef]

9.　Shangguan, P.; Al-Qadi, I.L.; Leng, Z.; Schmitt, R.L.; Faheem, A. Innovative approach for asphalt pavement compaction monitoring with ground-penetrating radar. *Transp. Res. Rec.* **2013**, *2347*, 79–87. [CrossRef]

10.　Daniels, D.J. *Ground Penetrating Radar*; Knoval, Institution of Engineering and Technology: New York, NY, USA, 2004; pp. 1–4. ISBN 978-0-86341-360-5.

11.　Leng, Z.; Al-Qadi, I.L.; Lahouar, S. Development and validation for in situ asphalt mixture density prediction models. *NDT E Int.* **2011**, *44*, 369–375. [CrossRef]

12.　Zhao, S.; Al-Qadi, I.L. Algorithm development for real-time thin asphalt concrete overlay compaction monitoring using ground-penetrating radar. *NDT E Int.* **2019**, *104*, 114–123. [CrossRef]

13.　Wang, H.; Wang, C.; You, Z.; Yang, X.; Huang, Z. Characterising the asphalt concrete fracture performance from X-ray CT Imaging and finite element modelling. *Int. J. Pavement Eng.* **2018**, *19*, 307–318. [CrossRef]

14.　Xiao, M.; Reddi, L.N.; Steinberg, S.L. Variation of water retention characteristics due to particle rearrangement under zero gravity. *Int. J. Geomech.* **2009**, *9*, 179–186. [CrossRef]

15.　Liu, P.; Xu, H.; Wang, D.; Wang, C.; Schulze, C.; Oeser, M. Comparison of mechanical responses of asphalt mixtures manufactured by different compaction methods. *Constr. Build. Mater.* **2018**, *162*, 765–780. [CrossRef]

16.　Chen, J.; Huang, B.; Shu, X. Air-void distribution analysis of asphalt mixture using discrete element method. *J. Mater. Civ. Eng.* **2013**, *25*, 1375–1385. [CrossRef]

17.　Qian, G.; Hu, K.; Li, J.; Bai, X.; Li, N. Compaction process tracking for asphalt mixture using discrete element method. *Constr. Build. Mater.* **2020**, *235*, 117478. [CrossRef]

18.　Wang, L.; Zhang, B.; Wang, D.; Yue, Z. Fundamental mechanics of asphalt compaction through FEM and DEM modeling. *Anal. Asph. Pavement Mater. Syst. Eng. Methods* **2007**, 45–63. [CrossRef]

19.　Shao, Y.U. Coupling analysis of FEM/DEM for whole failure process of rock slope and its engineering application. *J. Shanghai Jiaotong Univ.* **2013**, *47*, 1611.

20.　Guo, N.; Zhao, J. A coupled FEM/DEM approach for hierarchical multiscale modelling of granular media. *Int. J. Numer. Methods Eng.* **2014**, *99*, 789–818. [CrossRef]

21. Du, B.; Zhao, C.; Dong, G.; Bi, J. FEM-DEM coupling analysis for solid granule medium forming new technology. *J. Mater. Processing Technol.* **2017**, *249*, 108–117. [CrossRef]

22. Orosz, Á.; Zwierczyk, P.T. Analysis of the stress state of a railway sleeper using coupled FEM-DEM simulation. In *ECMS*; CRC Press: Boca Raton, FL, USA, 2020; pp. 261–265. ISBN 978-1-4665-8020-6.

23. Khennane, A. *Introduction to Finite Element Analysis Using MATLAB® and Abaqus*; CRC Press: Boca Raton, FL, USA, 2013.

24. Systèmes, D. *Abaqus Analysis User's Guide (6.14)*; Abaqus FEA: Providence, RI, USA, 2014.

25. Hertz, H. On the contact of solids—on the contact of rigid elastic solids and on hardness. In *Miscellaneous Papers*; Macmillan and Co.: New York, NY, USA, 1896; pp. 146–183.

26. Johnson, K.L.; Kendall, K.; Roberts, A. Surface energy and the contact of elastic solids. *Proc. R. Soc. Lond. A Math. Phys. Sci.* **1971**, *324*, 301–313.

27. Wang, X.; Shen, S.; Huang, H.; Almeida, L.C. Characterization of particle movement in Superpave gyratory compactor at meso-scale using SmartRock sensors. *Constr. Build. Mater.* **2018**, *175*, 206–214. [CrossRef]

28. Wang, C.; Moharekpour, M.; Liu, Q.; Zhang, Z.; Liu, P.; Oeser, M. Investigation on asphalt-screed interaction during pre-compaction: Improving paving effect via numerical simulation. *Constr. Build. Mater.* **2021**, *289*, 123164. [CrossRef]

29. Golalipour, A.; Jamshidi, E.; Niazi, Y.; Afsharikia, Z.; Khadem, M. Effect of aggregate gradation on rutting of asphalt pavements. *Procedia Soc. Behav. Sci.* **2012**, *53*, 440–449. [CrossRef]

30. Jin, C.; Zhang, W.; Liu, P.; Yang, X.; Oeser, M. Morphological simplification of asphaltic mixture components for micromechanical simulation using finite element method. *Comput. Aided Civ. Infrastruct. Eng.* **2021**, *36*, 1435–1452. [CrossRef]

31. Jin, C.; Wan, X.; Liu, P.; Yang, X.; Oeser, M. Stability prediction for asphalt mixture based on evolutional characterization of aggregate skeleton. *Comput. Aided Civ. Infrastruct. Eng.* **2021**, *36*, 1453–1466. [CrossRef]